Available online at www.sciencedirect.com
SCIENCE DIRECT®
International Journal of Thermal Sciences 43 (2004) 753–760
International Journal of Thermal Sciences
www.elsevier.com/locate/ijts

Effects of vortex organization on heat transfer enhancement by Görtler instability

Ladan Momayez, Pascal Dupont, Hassan Peerhossaini

Thermofluids and complex flows research group, laboratoire de thermocinétique – CNRS, UMR-6607, École polytechnique de l'université de Nantes, rue Christan Pauc, BP 90604, 44306 Nantes cedex 3, France

Received 20 August 2003; received in revised form 7 January 2004; accepted 24 February 2004

Available online 9 June 2004

Abstract

Görtler vortices, which appear due to streamline curvature in a boundary layer, drastically modify the momentum and heat-transfer properties of the boundary layer.

Görtler instability and, as such, heat transfer enhancement by Görtler instability are dependent on initial conditions. In particular, the upstream perturbation wavelength affects downstream nonlinear enhancement of the heat-transfer rate. In this paper we investigate this effect and show that the shorter wavelengths of the upstream perturbations increase the heat-transfer rate of nonlinear Görtler vortices.
© 2004 Elsevier SAS. All rights reserved.

Keywords: Hydrodynamic stability; Görtler instability; Centrifugal instability; Corrective heat transfer; Boundary layer transition; Thermal boundary layer

1. Introduction

Boundary layers with curved streamlines are susceptible to an instability mechanism of centrifugal type often called the Görtler instability [1]. The unstable regime consists of a laminar boundary layer over which an array of longitudinal vortices (Görtler vortices) is superposed. Görtler vortices are steady when they begin to appear. However, when the control parameter, the Görtler number G_θ , is increased, they undergo a secondary instability and eventual breakdown into turbulence.

1.1. Stability theory

The underlying physical mechanism for the instability of the boundary layer over a concave wall, which appears as the emerging of streamwise vortices, is similar to that shown by Rayleigh [2] for a rotating inviscid fluid and by Taylor [3] for a viscous fluid in the annulus between two rotating concentric cylinders. Rayleigh [2] stated that for the inviscid flow between two concentric coaxial cylinders, the outward increase of the circulation provides a sufficient condition for the onset of an instability. Validity of this statement for viscous fluids was proved later.

The circulation in a flow is locally determined by velocity of a particle and the curvature of its path-line. Thus the proper modelling of the instability mechanism requires knowledge of the velocity field and the geometry of the streamlines. This second factor had led to serious difficulties in the early attempts of the linear stability analysis of a concave boundary layer, and is the point where different analysis diverge from each other. Herbert [4] gives a review of these early works and the origin of their controversial predictions of the marginal stability curves.

Contrary to the curvature effects and its extents, the effect of the boundary layer growth appears explicitly in the governing equations through the normal-to-the-wall velocity term. The main difficulty in relation to these terms is the need to use an approximation for the curvature terms (in the stability equations) that is consistent with the approximation used. In the boundary layer equations Görtler [1] neglected some curvature terms which were not related to the approximation of the behaviour of the streamlines away from the wall. They contained components of the normal-to-the-wall velocity; Görtler predicted the threshold of instability for $G_\theta \cong 0.56$. Floryan and Saric [5] showed that, in the parallel flow approximation, the effect of these terms is insignificant. Smith [6] was the first to

E-mail address: hassan.peerhossaini@polytech.univ-nantes.fr (H. Peerhossaini).

1290-0729/$ – see front matter © 2004 Elsevier SAS. All rights reserved.
doi:10.1016/j.ijthermalsci.2004.02.015

Nomenclature

C_p	heat capacity	$\mathrm{J{\cdot}kg^{-1}{\cdot}K^{-1}}$
d_w	wire diameter	m
G_θ	Görtler number ($\frac{U_n\theta}{\nu}\sqrt{\frac{\theta}{R}}$)	
H	height of counter wall, $H = 0.15$	m
Pr	Prandtl number, $= \frac{\nu}{\kappa}$	
R	wall radius of curvature	m
Re	Reynolds number ($\frac{U_n x}{\nu}$)	
St	Stanton number ($\frac{\varphi_W}{\rho C_p U_{\mathrm{pw}}(T_{\mathrm{wall}}-T_\infty)}$)	
T_f	film temperature, $T_f = \frac{(T_p+T_\infty)}{2}$	K
T_∞	or T_{inf} free-stream temperature	K
T_w	wall temperature	K
U	streamwise component of velocity	$\mathrm{m{\cdot}s^{-1}}$
U_n	free-stream velocity or nominal velocity	$\mathrm{m{\cdot}s^{-1}}$
U_{pw}	potential wall velocity, $= \frac{U_n}{\frac{R}{H}\ln(1-\frac{H}{R})} \approx 0.88U_n$	$\mathrm{m{\cdot}s^{-1}}$
x	streamwise direction	m
y	normal to wall direction	m
z	spanwise direction	m

Greek symbols

α	wavenumber	$\mathrm{m^{-1}}$
β	dimensionless spatial amplification factor	
κ	thermal diffusivity	$\mathrm{m^2{\cdot}s^{-1}}$
λ	spanwise forced wavelength	m
Λ	wavelength parameter, $= \frac{U_\infty\lambda}{\nu}(\frac{\lambda}{R})^{1/2}$	
ν	kinematic viscosity	$\mathrm{m^2{\cdot}s^{-1}}$
ρ	density	$\mathrm{kg{\cdot}m^{-3}}$
φ_w	wall heat flux	$\mathrm{W{\cdot}m^{-2}}$
θ	Blasius momentum thickness, $= 0.664x(Re)^{-1/2}$	m

take the effect of normal-to-the wall velocity component into consideration. Floryan and Saric [5] used Smith's model and found that normal-to-the-wall terms in a growing boundary layer considerably destabilize the boundary layer, but this destabilization is more apparent than real due to one coordinate-related term missing from this model.

Naturally, the solution of the differential disturbance equations is simplified considerably by linearization for small disturbances. However, it is clear that the stability problem is inherently nonlinear, because the equations of motion are nonlinear. Nonlinear evolution of Görtler vortices was addressed by Hall [7]. He considered nonlinear development of finite amplitude disturbances in a non-parallel boundary layer. It was found that if the conditions are favourable for the growth of the disturbances, the finite amplitude solution which develops in the neighbourhood of the position where the disturbances were introduced, changes its structure farther downstream. This behavior was not confirmed by experiments (Swearingen and Blackwelder [8]; Peerhossaini and Wesfreid [9]), in which it was found that the wavelength of the Görtler vortices are very robust; they are fixed by the initial perturbations and do not evolve farther downstream.

Nonlinear development of Görtler vortices was computed by Sabry and Liu [10]. Starting with the velocity profiles from experiments of Swearingen and Blackwelder [8] as initial conditions, they solved nonlinear Naviers–Stokes equations in curvilinear coordinates. They used weak Görtler vortices as initial conditions, but the shape of the initial velocity profiles was borrowed from the linear stability analysis of Floryan and Saric [5]. They successfully reproduced numerically the mushroom shaped structures and velocity profiles of the experiment in a rather long downstream distance, before the secondary instability becomes important. Beyond this limit the numerical predictions do not agree with experiments. Details of the secondary stability can be found in Park and Huerre [11], Yu and Liu [12,13] and the references in these papers.

The nonlinear computations of Sabry and Liu [10] and the works which followed allowed predictions of heat and mass transfer occurred by Görtler instability and made it available to experimentation. This constitutes a basis for the analysis of heat transfer enhancement and in particular the effects of up-stream wavelength; which is the subject of this work.

Görtler vortices embedded in the boundary layer affect heat, mass, and momentum transfer between the solid wall and the fluid (Peerhossaini [14]). Therefore, the different characteristic parameters of the Görtler vortices, such as wavelength, upstream perturbation strength, etc. affect the wall heat transfer.

1.2. Transport theory

Transport mechanism in a concave boundary layer in the presence of longitudinal vorticity differs from that of a flat boundary layer mainly due to the extra advection in the plane normal to the streamwise direction. In a laminar boundary layer over a flat plate, heat transfer in the normal-to-the-wall direction is achieved by molecular diffusion, whereas in the presence of the Görtler vortice the transfer is dominated by advection resulted from the secondary velocity flow field. Incompressibly conditions require that the flow field and temperature field are uncoupled, and as such heat is transported as a passive quantity, by the flow field. In this case, as will be discussed below, the initial value of the temperature distribution does not affect the downstream enhancement of heat transfer by longitudinal vortices.

McCormac et al. [15] found that heat transfer between a curved heated wall (in uniform wall-heat-flux condition) and the boundary layer showed an increase of 30–190% (according to spanwise position), with an average of 110% beyond the flat wall Nusselt number. Nevertheless, there were too few spanwise measurement points to determine whether the spanwise distribution of Nusselt number was periodic or followed any regular waveform. Thus, only the global heat-transfer enhancement caused by the Görtler vortices could be deduced. McCormack et al. [15] also performed a linear stability analysis of the Görtler vortices based on which the Nusselt number was calculated for the same conditions as in the experiments. It was found that the ratio of the Nusselt number over flat-plate Nusselt number should vary sinusoidally. The amplitude of the waveform was 60% relative to the mean, but the spanwise averaged heat transfer enhancement was null. As expected the linear Görtler vortices enhance heat transfer rate in the down-wash regions and reduce it in the up-wash zones, the balance is zero. Therefore heat transfer enhancement can be expected only where the vortices have become nonlinear, downstream of their generation. This conclusion has a significant consequence, since in terms of longitudinal distance, linear growth occupies almost half of the vortex development length, before break-down to turbulence (Peerhossaini and Bahri [16]). Heat transfer experiments of Crane and Umur [17] performed in a curved water channel confirmed that the spanwise-averaged Stanton number exceeded the analytic value of the flat-plate Stanton number only in the highly nonlinear (and probably turbulent) Görtler vortex regime. The Görtler number beyond which the heat transfer enhancement became observable was $G_\theta = 10$. This observation is in agreement with the findings of the present work in which we have progressively increased the instability control parameter (the Görtler number) and have observed the gradual increase of heat transfer enhancement by the Görtler vortices beyond the linear regime.

A physical explanation of heat transfer enhancement in the nonlinear regime comes from the numerical simulations of Liu and Lee [18] for strong nonlinear Görtler vortex development, as well as the velocity field measurements of Peerhossaini and Bahri [16]. These works have shown that in the nonlinear regime the down-wash region in the boundary layer (with sharp velocity gradient in the wall vicinity) is wider than the up-wash region where the velocity gradient is milder. Therefore the sites of heat transfer increase (compared to the flat-plate boundary layer) are more extended than those of heat transfer reduction, resulting in a positive net heat transfer enhancement. Computations of Benmalek and Saric [19] show the same trend as those found by Peerhossaini and Bahri [16] for the streamwise evolution of the spanwise profiles of the streamwise velocity in the nonlinear Görtler vortex regime.

Following the nonlinear development of Görtler vortices introduced by Sabry and Liu [10], Liu and Lee [18] solved the equations for heat transport by the Görtler vortices in the same configuration as in Sabry and Liu [10]. Due to the incompressibility assumption and for low heat loading the momentum and energy equations are decoupled. Therefore, once the momentum equation is solved the energy equation becomes a simple advection-diffusion equation with the instability constraints imposed on the momentum equation. This approach allowed the authors to investigate the effects of momentum and temperature initial conditions on the heat transfer enhancement by the Görtler vortices in the nonlinear regime.

Liu and Lee [18] studied the effects of wavelength and amplitude of the initial velocity perturbations as well as the amplitude of the initial temperature profile on heat transfer rate. They found that momentum initial conditions have a strong impact on heat transfer rate in the downstream, where as the temperature profile has a negligible effect. Their results will be discussed in relation with the experimental results of the present work.

Görtler instability is initial conditions-dependant and as such upstream perturbation parameters such as initial-perturbation wavelength and strength can be used as actuator parameters in the active control of heat and mass transfer. This is one of the long term aims of this work, and the results presented here constitute a preliminary step in this direction.

The wavelength of the Görtler vortices is a robust parameters. It is determined by the incipent Görtler vortices generated in the linear region and remains constant up to the break-down of the vortices. However, the Görtler instability does not have a wavelength selection mechanism; it is generally determined by some upstream device such as honey combs of the settling chamber (of the wind or water tunnel) or roughness elements. Therefore, the Görtler number defined as $G_\theta = \frac{U_\infty \theta}{\nu}(\frac{\theta}{R})^{1/2}$ can be recasted as $G_\theta = \Lambda(\alpha\theta)^{3/2}$ in which Λ is called the wavelength parameter and defined as $\Lambda = \frac{U_\infty \lambda}{\nu}(\frac{\lambda}{R})^{1/2}$. For a given freestream velocity and λ, the value of Λ remains constant all the way downstream in the unstable boundary layer, up to the break-down of the vortices to turbulence. The lines of constant Λ value appear as straight lines of slop $3/2$ on the stability diagram ($G_\theta - \alpha\theta$ plane). Lines of constant Λ value obtained experimentally are located in the amplified (and even highly amplified) region of the linear stability analysis, since Görtler vortices are not detectable close to the stability threshold ($G_\theta \cong 0.46$ according to the linear stability analysis of Floryan and Saric [5]).

In this paper we report on a heat-transfer study of the Görtler vortices forced by an array of wires fixed upstream of a concave boundary layer. By changing the distance between the forcing wires we controlled the wavelength of the Görtler vortices generated in the curved boundary layer under Görtler instability, and we investigated their effects on the wall heat transfer. The Stanton number was used to examine the relation between the vortex wavelength and the wall heat transfer. We discuss this relation for different Görtler numbers.

The rest of this paper is organized as follows. Section 2 describes the experimental apparatus in which this investigation is performed. Results are presented and discussed in Section 3 and concluding remarks in Section 4.

2. Experimental apparatus

Experiments were carried out on the concave boundary layer developed in a concave-convex model mounted in a laminar open-loop wind tunnel. More details on the wind tunnel and concave-convex model used in this work can be found in Peerhossaini and Bahri [16]. The nominal freestream velocity could vary between 1.5 and 10 $\mathrm{m \cdot s^{-1}}$ with constant turbulence intensity 0.7%.

The concave-convex model shown in Fig. 1 has four main parts:

– the leading edge in the shape of a thick laminar airfoil (NACA-0025),
– the concave part (radius of curvature 65 cm) in which measurements were carried out,
– the convex part (radius of curvature 15 cm),
– the trailing edge, a flat plate that can rotate around the center of curvature of the convex section.

The origin of the curvilinear axial coordinate x is fixed at the leading edge, and the concave wall starts at $x =$ 9 cm. It has been shown that Görtler instability does not have a natural wavelength selection mechanism. Görtler vortices are generated as the result of the amplification by centrifugal instability of upstream perturbations entering the concave boundary layer. In this study the spanwise position of the Görtler vortices was fixed by forcing predetermined wavelengths upstream of the leading edge. This was done by a perturbation grid made of 0.18 mm diameter wires with different wavelengths placed vertically exactly 4 mm upstream of the leading edge. The perturbation grid consists of a metallic rectangular frame on the lower and upper horizontal sides of which several holes (of constant inter-hole distance) are made. The distance between the holes fixes the perturbation wavelength. A plastic wire of 0.18 mm runs through the upper and lower holes and makes a grid of several vertical bars (wires). The frame is fixed vertically upstream of the test model. Perturbations generated in the wake of the grid wires are then injected by the flow in to the boundary layer which develops on the concave wall. Amplification of these perturbations by Görtler instability mechanism gives rise to the appearance of the Görtler vortices. Grids with different wire distances were used to force perturbations of different wavelengths.

The model surface was covered with a thin (130 µm) resistance film composed of a 70 µm Constantan layer glued to a 60 µm Kapton film and was heated by the Joule effect. 196 Chromel–Alumel thermocouples of 80 µm bead measured the temperature on the Kapton side of the heating film.

In order to reduce heat loss from the back side of the model wall, it was insulated with Phenolic foam ($k =$ 0.02 $\mathrm{W \cdot m^{-1} \cdot K^{-1}}$) in which eight thermocouples were implanted. Measurements showed that heat losses by conduction from the back side of the model were 6–8 $\mathrm{W \cdot m^{-2}}$, that is between 3 and 4% of the imposed flux.

3. Stanton number variation with vortex wavelength

3.1. Heat transfer enhancement

Experiments were run at nominal freestream velocities of $U_n = 2, 3, 4.8, 7$, and 9 $\mathrm{m \cdot s^{-1}}$ and wall heat flux of $\varphi_p = 200$ $\mathrm{W \cdot m^{-2}}$. The forced wavelength varied between 2.5 and 30 mm in increments of 5 mm. Fluid velocity and temperature were measured respectively by a Pitot tube and a platinum probe, both in the freestream. The local wall temperature field was measured by the wall thermocouples and Stanton number was calculated from these data.

Fig. 2 shows the evolution of Stanton number versus Görtler number for various spanwise forced wavelengths and freestream velocity 3 $\mathrm{m \cdot s^{-1}}$, where the correlations for laminar and turbulent boundary layer are also superposed (Kays and Crawford [20]):

$$St = 0.453 Pr^{-2/3} Re_x^{-1/2} \quad \text{for laminar boundary layer}$$
$$St = 0.03 Pr^{-0.4} Re_x^{-0.2} \quad \text{for turbulent boundary layer}$$

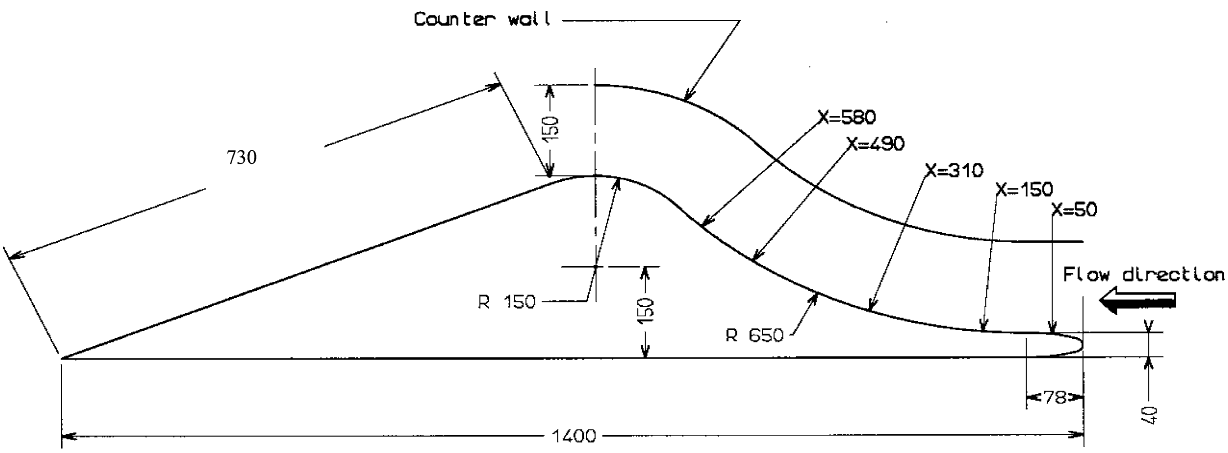

Fig. 1. Schematic diagram of the model.

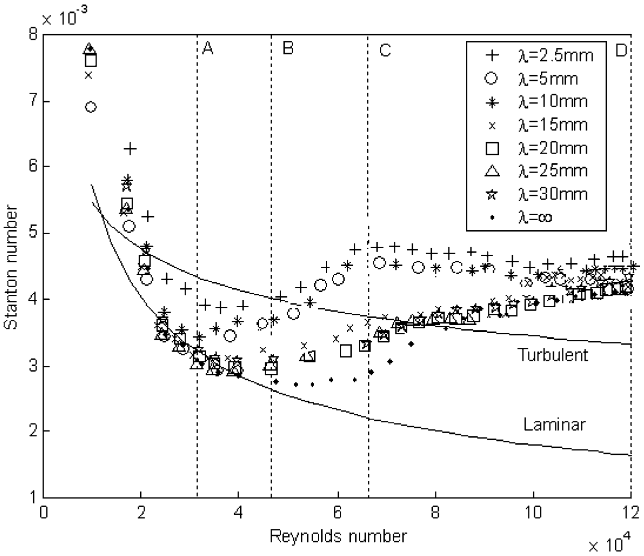

Fig. 2. Effects of forcing wavelength on the evolution of the Stanton number versus Reynolds number for $U_n = 3\ \text{m}\cdot\text{s}^{-1}$ and $d_w = 0.18$ mm.

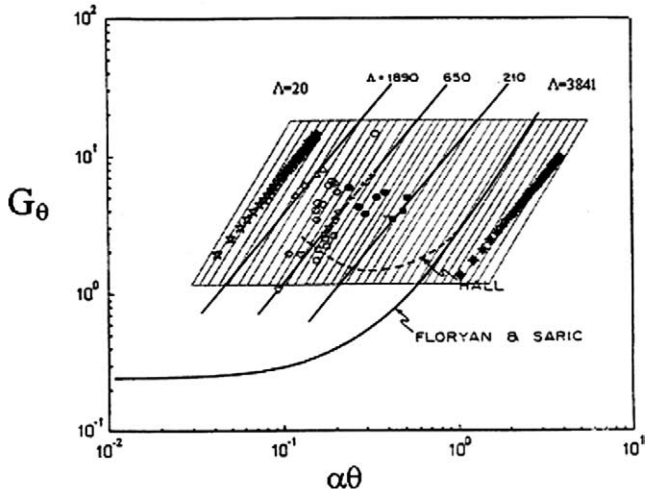

Fig. 3. Experimental domains are shown by constant-value Λ lines: ($*$) present work with $U = 2\ \text{m}\cdot\text{s}^{-1}$, $\lambda = 2.5$ mm; (★) present work with $U = 9\ \text{m}\cdot\text{s}^{-1}$, $\lambda = 30$ mm; (+) Swearingen and Blackwelder; (●) Winoto and Crane; (■) Bippes; (□) Tani $R = 5$ m, $U = 3\ \text{m}\cdot\text{s}^{-1}$; (○) Tani $R = 5$ m, $U = 7\ \text{m}\cdot\text{s}^{-1}$; (△) Tani $R = 5$ m, $U = 13\ \text{m}\cdot\text{s}^{-1}$; (▽) Tani $R = 10$ m, $U = 11\ \text{m}\cdot\text{s}^{-1}$; (◇) Tani $R = 10$ m, $U = 16\ \text{m}\cdot\text{s}^{-1}$; Floryan and Hall marginal stability curves are also shown.

In Fig. 2 the experimental points closely follow the curve of the flat boundary layer for Görtler numbers smaller than $G_\theta \approx 3.6$. However, beyond this control-parameter value, the experimental results deviate from the theoretical laminar flat-plate boundary layer, revealing the effects of the Görtler vortices on the wall heat transfer.

3.2. Effects of the initial perturbation wavelength

Our understanding of Görtler instability has progressed continuously ever since Görtler's pioneering work in 1940, in which for the first time counterrotating vortices were hypothesized in an open wall-bounded system. Probably the most decisive conclusion, from the fundamental point of view, is the dependence on initial conditions of the instability growth and breakdown mechanism of the Görtler vortices. The outcome has been the emphasis placed in recent years on the receptivity problem (see Saric et al. [21] for a comprehensive review), where the aim is to understand the source of the initial disturbances rather than the details of later developments.

Görtler instability has been shown to be initial-condition dependent (Hall [7]). Sabry and Liu [10] showed numerically that the downstream nonlinear development of momentum, heat and mass transfer are closely related to the initial conditions imposed on the flow.

The wavelength and strength of the initial perturbations are among the dominant parameters affecting the nonlinear development of Görtler vortices and hence heat-transfer enhancement. This property gives particular importance to these parameters for active control of heat (and mass and momentum) transfer in many applications of technological importance.

The wavelength of incipient Görtler vortices fixes their wavelength throughout their nonlinear development and breakdown to turbulence. Vortex evolution in the $G_\theta - \alpha\theta$ stability diagram thus follows the power law $G_\theta = \Lambda_\lambda(\alpha\theta)^{3/2}$. Detectable Görtler vortices (by measurement of their velocity field and other signatures) are all located in the highly amplified region of the stability diagram, as shown in Fig. 3. According to the linear theory, Görtler vortices are amplified more or less depending on their position in relation to the curve of maximum linear amplification.

In the present work, vortices in a large range of wavelength parameter Λ_λ were generated and the evolution of their spanwise averaged Stanton number with Görtler number was investigated. The wavelength parameter varied from 20 in the unamplified region of the stability diagram, to 3841 in the weakly amplified nonlinear zone. This range, shown by parallel lines in Fig. 3, exceeds that in all previous experiments reported in the open literature. Table 1 gives the numerical values of Λ_λ corresponding to each (λ, U_n) pair.

From the Stanton–Görtler curves for different nominal flow velocities (2, 3, 4.8, 7 and 9 $\text{m}\cdot\text{s}^{-1}$; Fig. 4 shows an example of these curves for $U_n = 3\ \text{m}\cdot\text{s}^{-1}$) two distinct behaviours appear:

- curves with $\lambda < 10$ mm, which group together and show a higher heat-transfer enhancement,
- curves with $\lambda \geqslant 15$ mm, which also group together and include as well the unforced wavelength (without the wavelength-triggering grid) case (which is in reality of infinite wavelength); this second group shows lower heat-transfer enhancement than the first.

It seems that the natural perturbations (no wavelength forcing) constitute the finite lower bound for advection heat-transfer enhancement (Momayez et al. [22]). However, as

Table 1
Range of Λ parameter covered in the present study

U	λ						
	2.5 mm	5 mm	10 mm	15 mm	20 mm	25 mm	30 mm
2 m·s^{-1}	20	58	164	301	465	649	854
3 m·s^{-1}	31	87	246	453	697	974	1280
4.8 m·s^{-1}	49	139	394	724	1115	1558	2049
7 m·s^{-1}	72	203	575	1056	1626	2273	2988
9 m·s^{-1}	92	261	739	1358	2091	2922	3841

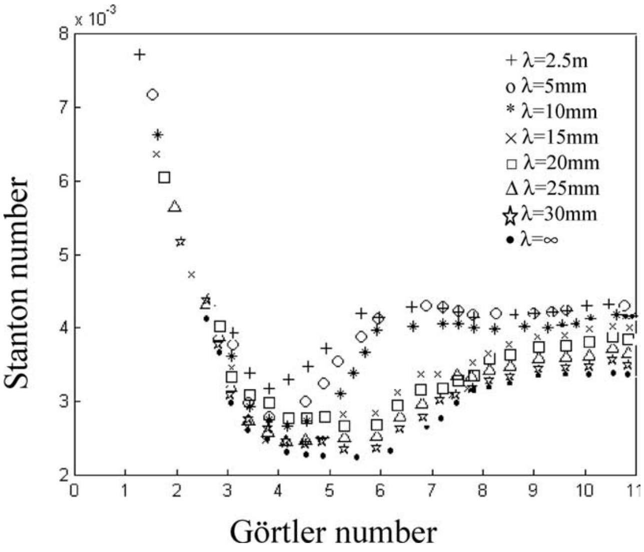

Fig. 4. Effect of forcing wavelength on the evolution of the Stanton number versus Görtler number for $U_n = 3$ m·s^{-1}, $d_w = 0.18$ mm.

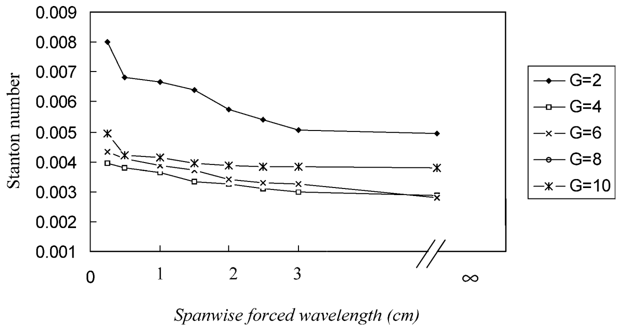

Fig. 5. Evolution of Stanton number versus wavelength number for $U_n = 3$ m·s^{-1}, $d_w = 0.18$ mm.

shown in Fig. 4 (and those for other U_n's), at higher Görtler numbers ($G_\theta > 6$ for $U_n = 3$ m·s^{-1}) the Stanton-number curve departs from that of the laminar boundary layer and approaches the Stanton-number curve for the turbulent flat-plate boundary layer.

Except for $\lambda = 2.5$ mm and $U_n = 2$ m·s^{-1} ($\Lambda_\lambda \approx 20$), the wavelength parameters Λ_λ of the curves of the first group vary between 100 and 500; around the maximum amplification range in linear theory. The wavelength parameters of the second group vary between 500 and 3800; their values have a very weak effect on the Stanton number. The weak variation of the Stanton number with Λ_λ in this range is principally due to the sparseness of the Görtler vortices with respect to the model width, in addition to their slower growth rate in the nonlinear region. In a numerical experiment, Liu and Sabry [23] increased the wavelength of the incipient Görtler vorticies by a factor of two, thus increasing the wavelength parameter Λ_λ (initial value $\Lambda_\lambda = 460$) by a factor of almost three. The perturbation amplification thereby decreased and effected a smaller wall heat-transfer enhancement compared to the initial case ($\lambda = \infty$).

The variation of Stanton number with λ is better captured in Fig. 5, in which St is plotted against λ with G_θ as a parameter. Except for the curve $G_\theta = 2$ it can be seen that for a given wavelength, wall heat transfer increases with increasing Görtler number, due to the stronger nonlinear amplification of the vortices. The case $G_\theta = 2$ corresponds to the zone close to the leading edge, where the boundary layer is thin and much more heat is transferred from the wall to the boundary layer.

For other Görtler numbers, heat transfer enhancement is up to 25% greater at low wavelengths, whatever the amplification state of the vortices. It asymptotically approaches the value for the infinite-wavelength limit.

At the high-Görtler-number end, vortex wavelength has a very moderate effect; heat transfer is insensitive to the wavelength, as is evident in Fig. 5 for $G_\theta = 10$. In fact, from $G_\theta > 6.9$, time dependence sets in through secondary instability (Momayez et al. [22]); the meandering motion of the vortices makes the spanwise wavelength a less meaningful spatial barrier between neighbouring vortices. It was clearly shown in the flow visualizations of Peerhossaini and Wesfreid [9] that this mechanism is strongly Görtler-number-dependent. The frequency and amplitude of the vortex oscillation increase with Görtler number augmentation; the smaller the frequency and amplitude, the greater the wavelength effect. In some very-high-Görtler-number values before vortex breakdown, a vortex dynamic sets in that is quite challenging to model: the downwash part of one vortex is attracted to and swallowed by the upwash part of the neighbouring vortex. This mode, referred to as "attraction and swallow" and shown in Fig. 6, completely undermines the wavelength notion: it generates a strong sweeping action on the wall and very intense mixing in the wall shear layer by vortex mingling. The consequence is a strong heat-transfer enhancement.

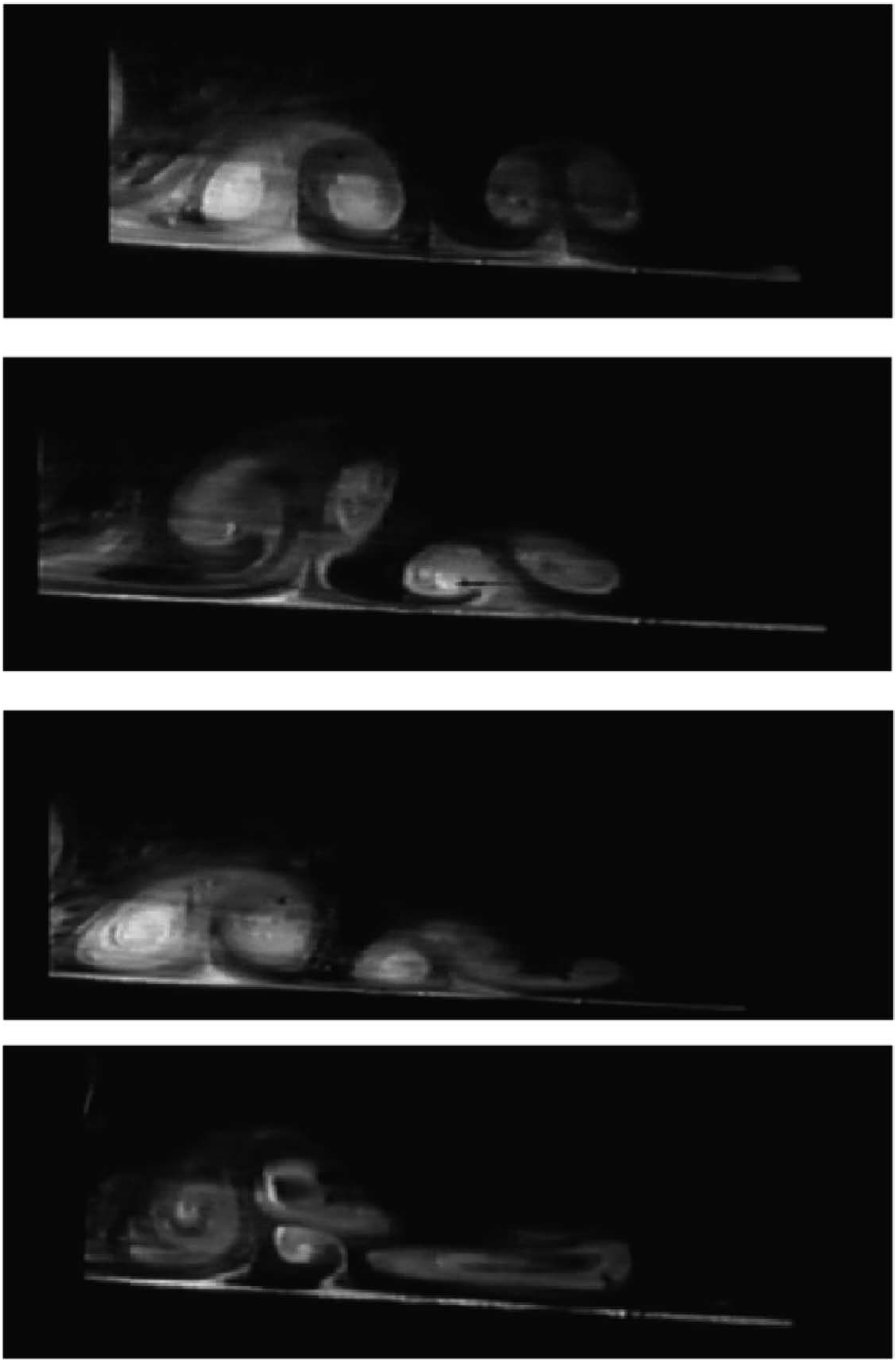

Fig. 6. Attraction and swallow process.

After the complete breakdown of the vortices, a fine-grained turbulence sets in which disintegrated parts of large vortex structures appear intermittently (Peerhossaini and Wesfried [9]). This is the case for $G_\theta > 9$ in which Stanton curves of vortices with different wavelength collapse, as seen in Fig. 4. Physically, this merging means that, unlike the nonlinear vortex growth in which the past history of vortices is preserved, once broken in turbulence, wavelength memory is smeared; the only remnant of vortices of all wavelengths is the intermittent vorticity spots that enter from upstream flow to the turbulent zone. Notice that in Fig. 5 the $G_\theta = 6$ and $G_\theta = 8$ curves completely overlap and the curve for $G_\theta = 10$ becomes an almost horizontal line parallel to the wavelength axis.

4. Concluding remarks

A concave-convex model has been constructed and tested in a low-turbulence wind tunnel to investigate the effects of Görtler vortices on the wall heat-transfer rate. Görtler vortices were generated by a centrifugal instability mechanism referred to as the Görtler instability.

We showed that heat transfer by Görtler vortex is sensitive to upstream conditions. Effects of upstream perturbation wavelength were closely studied. It was found that the wavelength of the incipient Görtler vortices expressed as the wavelength parameter Λ_λ has a definite effect on heat-transfer enhancement. If the wavelength parameter of the vortices is close to the zone of maximum linear amplification in the stability diagram, heat-transfer amplification is higher.

References

[1] H. Görtler, On the three-dimensional instability of laminar boundary layers on concave walls, Nacher, Ges. Wiss. Göttingen (NACA TM 1375) 2 (1954) 1–26.

[2] L. Rayleigh, On the dynamics of revolving fluids, Scientific Papers 6 (1916) 447–453.

[3] G.I. Taylor, Stability of a viscose liquid contained between rotating cylinders, Philos. Trans. Roy. Soc. London A 223 (1923) 289–343.

[4] Th. Herbert, On the stability of the boundary layer along a concave wall, Arch. Mech. Warszawa 28 (5–6) (1976) 1049–1055.

[5] J.M. Floryan, W.S. Saric, Stability of Görtler vortices in boundary layers, AIAA J. 20 (1982) 316–324.

[6] A.M.O. Smith, On the growth of Taylor–Görtler vortices along highly concave walls, Quart. J. Math. 13 (1955) 2333–2362.

[7] P. Hall, The linear development of Görtler vortices in growing boundary layer, J. Fluid Mech. 130 (1983) 41–58.

[8] J.D. Swearingen, R.F. Blackwelder, The growth and break-down of streamwise vortices in the presence of a wall, J. Fluid Mech. 182 (1987) 255–290.

[9] H. Peerhossaini, J.E. Wesfreid, On the inner structure of Görtler vortices, Internat. J. Heat Fluid Flow 9 (1988) 12–18.

[10] A.S. Sabry, J.T.C. Liu, Longitudinal vorticity elements in boundary layers: Non-linear developments from initial Görtler vortices as a prototype problem, J. Fluid Mech. 231 (1991) 615–663.

[11] D.S. Park, P. Huerre, Primary and secondary instabilities of the asymptotic suction boundary layer on a curved plate, J. Fluid Mech. 283 (1995) 249–272.

[12] X. Yu, J.T.C. Liu, The secondary instability in Görtler flow, Phys. Fluids A 3 (1991) 1845.

[13] X. Yu, J.T.C. Liu, On the mechanism of sinuous and varicose modes in three-dimensional viscous secondary instability of nonlinear Görtler rolls, Phys. Fluids 6 (1994) 736.

[14] H. Peerhossaini, On the effects of streamwise vortices on wall heat transfer, in: R. Shah (Ed.), Compact Heat Exchangers for Process Industries, Begell House, New York, 1997, pp. 571–589.

[15] P.D. McCormack, H. Wellker, M. Kelleher, Taylor–Görtler vortices and their effect on heat transfer, ASME J. Heat Transfer 92 (1970) 101.

[16] H. Peerhossaini, F. Bahri, On the spectral distribution of the modes in non-linear Görtler instability, Experimental Thermal Fluid Sci. 16 (1998) 195–208.

[17] R.I. Crane, H. Umur, Concave wall laminar heat transfer and Görtler vortex structure: effect of pre-curvature boundary layer and favourable pressure gradients, ASME, Paper No. 90-GT-94, 1990.

[18] J.T.C. Liu, K. Lee, Heat transfer in a strongly non-linear spatially developing longitudinal vortices system, Phys. Fluids 7 (1995) 559–599.

[19] A. Benmalek, W.S. Saric, Effect of curvature variations on the non-linear evolution of Görtler vortices, Phys. Fluids 6 (10) (1994) 3353–3354.

[20] W.M. Kays, M.E. Crawford, Convection Heat and Mass Transfer, third ed., McGraw-Hill, New York, 1993.

[21] W.S. Saric, H.L. Reed, E.D. Kerschen, Boundary-layer receptivity to freestream disturbances, Annual Rev. Fluid Mech. 34 (2002) 291–319.

[22] L. Momayez, P. Dupont, H. Peerhossaini, Some unexpected effects of wavelength and perturbation strength on heat transfer enhancement by Görtler instability, Internat. J. Heat Mass Tranfer, in press.

[23] J.T.C. Liu, A.S. Sabry, Concentration and heat transfer in nonlinear Görtler vortex flow and the analogy with longitudinal momentum transfer, Proc. Roy. Soc. London 432 (1991) 1–12.